THE DUCTILE FRACTURE MECHANISM IN RARE-EARTH-TREATED HSLA STEELS

J. D. Boyd and K. M. Pickwick*

INTRODUCTION

The generally accepted mechanism for ductile fracture is the void-nucleation-growth-coalescence model [1]. For structural steels (yield strength ≃300-700 MPa), the predominant void-nucleation sites are manganese sulphide inclusions which typically have an inter-particle spacing of approximately 50 μm. The fracture surfaces of such steels are characterized by dimples which have diameters comparable to the spacing of the MnS inclusions. In addition, dimples approximately 1 μm in diameter are often observed, and these are attributed to voids formed at small oxide inclusions [2]. The complete fracture process involves the nucleation of voids at both size groups of inclusions, but it is not clear what is the relative importance of the two size groups on the overall fracture toughness of the material [3, 4].

It has been shown that for steels with sulphur contents greater than approximately 0.004 wt. pct., the sulphide inclusions have the dominant effect on ductile fracture toughness (as indicated by the Charpy shelf energy) [5]. Thus, one of the trends in the development of high-toughness HSLA steels (e.g. for linepipe), has been the lowering of the permissible sulphur content to the 0.004-0.006 wt. pct. range, which effects a corresponding decrease in the volume fraction of sulphide inclusions. The practice of making additions of rare-earth metals (RE) to reduce the anisotropy of toughness in rolled plate has also been introduced. Other alloy development trends for this product include lower carbon content (down to 0.05 wt. pct.), and the universal adoption of fully deoxidized steel. Since the oxygen solubility varies inversely with the carbon content, more deoxidation is required for the lower carbon steels and an increased volume fraction of deoxidation product in the form of small oxide inclusions is expected. It is difficult to verify this metallographically because the size range of these oxide inclusions ($\gtrsim$1 μm) exceeds the resolution of the optical microscope, which is the traditional instrument for characterizing inclusion distributions in steel. Nevertheless, it seems reasonable to suggest that in the near future the size distribution and void-nucleating characteristics of small oxide inclusions could be the dominant factor in the ductile fracture of commercial linepipe steels.

Accordingly, a laboratory study has been carried out to assess qualitatively the role of inclusions in the ductile fracture of a representative low carbon, low sulphur, RE-modified linepipe steel. The objective was to identify the important void-nucleating sites, and to correlate the size distribution of inclusions with the impact toughness or ductility.

*Physical Metallurgy Research Laboratories, CANMET, Department of Energy, Mines and Resources, Ottawa, Canada.

EXPERIMENTAL

A low carbon-manganese-molybdenum-niobium composition was selected as suitable experimental material for this investigation. This composition is representative of the lowest carbon steels currently being used, in the as-rolled condition, for linepipe with a yield strength in the 450-500 MPa range.

The experimental material was prepared as two heats in a 225 Kg electric arc furnace with electrolytic iron as starting material, and using a two-slag practice. The steel was deoxidized in the furnace with Al and Si, and the Nb additions were made to the ladle as ferro-niobium. Additions of rare-earth metals, in the form of RE silicides, were made to the mould for one of the heats. Both heats were vacuum stream cast into a single 150 mm square mould, and the ingots were each cut into four slabs approximately 75 x 150 x 300 mm. The complete analyses for samples taken from the middle of the ingots are given in Table 1.

The slabs were upset-forged through the 150 mm dimension to 64 mm and then controlled rolled to 13 mm plate, finishing at approximately 800°C. In this way, the total reduction during hot working was 90 pct. with 20 pct. of the total reduction below 900°C. The transverse and longitudinal tensile properties of the rolled plate were similar for the two steels (Table 2), as was the microstructure, (a mixture of polygonal ferrite and acicular ferrite grains). Thus, for the subsequent comparisons between the two steels with respect to impact energy and fracture morphology, the yield strength and microstructure was taken to be constant.

Tests were also made on a commercial Mn-Mo-Nb steel which was obtained in the form of 17-mm plate. The chemical analysis and tensile properties of this material, as supplied by the producer, are also included in Tables 1 and 2 respectively. The microstructure of the commercial plate was also a mixture of polygonal ferrite and acicular ferrite, with a much finer grain size than the laboratory steels.

The experimental programme consisted of determining the type and distribution of inclusions in each of the steels and correlating these observations with measurements of toughness and ductility, and with observations of fracture-surface morphology. The distribution of inclusions was characterized by optical microscopy, and the various types of inclusions were identified using an X-ray microanalyser and an energy-dispersive X-ray analyser in conjunction with scanning electron microscopy (SEM). Complete impact energy transition curves were determined using longitudinal and transverse Charpy specimens, and the fracture surfaces of Charpy and tensile specimens were examined by SEM. Some tensile specimens were prepared with flat faces which were metallographically polished prior to testing. This made it possible to simultaneously examine the polished surface and the fracture surface in the SEM, which facilitated the correlation between inclusions and features on the fracture surface.

RESULTS

The complete impact energy transition curves are shown in Figure 1. The important observation from these data is that the impact energies for the ductile fracture mode, as indicated by the upper shelf energies, varied in the expected way. That is, the impact energies at 23°C for the RE-treated steel were similar for longitudinal and transverse specimens, and

fell between the longitudinal and transverse values for the untreated steels. At lower test temperatures there was much more scatter in the data, and there was no significant difference in the impact energy values for the four conditions. Data for the commercial Mn-Mo-Nb steel is also included in Figure 1 for comparison with the laboratory steels.

Optical metallography showed differences in the type and distribution of inclusions for the three steels (Figure 2). The untreated steel contained mostly duplex oxide/sulphide inclusions, with the sulphide inclusions often elongated in the rolling direction (Figure 2a@A), and isolated elongated sulphide inclusions (Figure 2a@C). The oxide inclusions were identified as silicates and alumina, and the sulphides were manganese sulphide. The RE-treated steel also contained duplex oxide/sulphide inclusions and isolated sulphides (Figure 2b), but in this case the sulphides were always equiaxed RE-oxysulphides. The commercial Mn-Mo-Nb steel appeared to be cleaner than the laboratory steels (i.e. fewer inclusions per unit area), and to contain mostly equiaxed RE-oxysulphides (Figure 2c).

The fracture surfaces of all tensile and Charpy specimens exhibited a 100 per cent dimpled morphology, which is indicative of the void-nucleation-growth-coalescence fracture mechanism. Although there was a wide range of dimple sizes observed, two distinct size groups were identified. Most of the dimples were 5-20 μm in diameter, but there were also clusters of much smaller dimples, 1-2 μm in diameter (e.g. Figure 3a@C). In the RE-treated steel the 5-20 μm dimples often contained equiaxed inclusions which were identified as RE-oxysulphides, (e.g. Figure 3b). Small equiaxed inclusions were often observed in the small dimples, (e.g. Figure 3c). These were also identified as RE-oxysulphides. For both size groups of dimples, the dimple diameter was 3-5 times that of the inclusion contained in it. Stereomicroscopy of transverse and longitudinal orientations revealed that many of the dimples, especially those in the 1-2 μm group, were highly elongated (Figure 3c).

The fracture morphology of the untreated steel was essentially similar to that of the RE-treated steel, except that many fewer inclusions were observed on the fracture surfaces. No elongated MnS inclusions were observed on the fracture surfaces, but there were some very large (20 μm X100 μm) elongated dimples. The fracture morphology of the commercial Mn-Mo-Nb steel was also similar to the others, and very few inclusions could be found on the fracture surfaces.

Some void-nucleating processes were observed on the polished surfaces of tensile specimens which could be significant to the overall fracture mechanism. In the RE-treated steel, clusters of small oxide and sulphide inclusions often occurred, and these could result in the nucleation of a large (25 μm) void in the necked region (Figure 4a). No inclusion-nucleated voids were observed on the polished surfaces of specimens of the untreated steel, but there was evidence of voids forming in regions of high local strain, i.e., slip bands (Figure 4b).

DISCUSSION

The Charpy impact data indicates that, even at the low sulphur levels and the low total reductions achieved in these experiments, RE additions have a significant effect on the anisotropy of ductile fracture energy, which can be attributed to inclusion shape modification. However, there are no corresponding differences in the fracture surface morphology, except

for the appearance of some elongated voids in the untreated steel, which may be related to elongated MnS inclusions.

The dominant features in the ductile fracture mechanism for all the steels studied are the 5-20 μm-diameter voids, and these appear to be nucleated by MnS or RE-oxysulphide inclusions. These voids generally impinge on each other, indicating that the fracture mechanism consists of nucleation of voids at optically-visible inclusions, followed by their growth and direct coalescence. There are isolated clusters of small, 1-2 μm-diameter voids, but these do not appear to play a major role in the fracture process. The nucleation sites for the small voids were not positively identified, but they appear to be small oxide or RE-oxysulphide inclusions. The size range of the particles observed in the small voids (0.1-0.5 μm), is also similar to that for grain-boundary carbides which occur in low-carbon HSLA steels.

The fact that the diameter of each dimple which contained an inclusion was 3-5 times the diameter of the inclusion indicates that large plastic strains are required for the nucleated voids to grow to the point of coalescence. This is consistent with geometric model of Brown and Embury [6], which predicts that a true plastic strain of approximately 5.4 is required for void growth when the void-nucleating sites are square-lattice array of particles whose volume fraction is 10^{-3}. The required strain must be achieved by localized plastic deformation on either the macro-scale (necking), or the micro-scale (slip bands). According to plasticity theory [7], a triaxial stress state is necessary for void growth, and this was confirmed by prestraining specimens to various strains at 23°C and then breaking them in liquid nitrogen. This experiment showed that appreciable void growth does not occur in tensile specimens until the latter stages of necking. There was also considerable evidence of localized plastic deformation on the micro-scale in the necked region (Figure 4). All of these factors support the thesis that extremely large plastic strains are required for failure to occur by the ductile fracture mechanism. It follows then, that failure can be averted in structures by limiting the maximum displacement by suitable design.

As far as the low-carbon-RE-treated steel is concerned, the results indicate that at the 0.05C and 0.005S level, sulphides are still the dominant microstructural features in the ductile fracture process. The laboratory-melted, RE-treated steels did contain some clusters of oxide inclusions which would be detrimental to toughness, but this could probably be avoided by careful steelmaking practice, and indeed no such clusters were observed in the commercial plate. However, the original premise still holds, that with further decreases in carbon content and volume fraction of sulphide inclusions, sub-micron size particles will become increasingly important in the fracture mechanism. Even at current carbon and sulphur levels, these particles could become the principal void formers if the yield strength of the matrix is increased by alloying or heat treatment. At higher strength levels, voids will nucleate at sub-micron particles at smaller strains than in the present experiments, and the required strain for void coalescence, according to the Brown-Embury model, will decrease rapidly as the volume fraction of void-forming particles increases.

In summary, impact energies and the details of the ductile fracture mechanism have been investigated for RE-treated and untreated, low-carbon, low-sulphur steels at constant yield strength and microstructure. It has been shown that optically-visible inclusions (usually MnS or RE-oxysulphides) are the predominant void-nucleating particles in these

steels, but it is expected that sub-micron oxide inclusions would become increasingly important at lower carbon or sulphur contents and higher yield strengths. The observations indicate that extremely large plastic strains are necessary for ductile fracture.

ACKNOWLEDGEMENTS

The assistance of D. E. Parsons and R. H. Packwood with the preparation of the laboratory steels and the X-ray microanalysis, respectively, is gratefully acknowledged.

REFERENCES

1. ROSENFIELD, A. R., Met. Revs., 13, 1968, 29.
2. KOZASU, I., SHIMIZU, T. and KUBOTA, H., Trans. Iron and Steel Inst. of Japan, 13, 1973, 20.
3. BROEK, D., Eng. Fract. Mech., 5, 1973, 55.
4. THOMPSON, A. W. and WEIHRAUCH, P. F., Scripta Met., 10, 1976, 205.
5. GRAY, J. M., Int. J. Pres. Ves. and Piping, 2, 1974, 95.
6. BROWN, L. M. and EMBURY, J. D., Proc. Third Int. Conf. on Strength of Metals and Alloys, Inst. of Metals, Cambridge, 1973, 164.
7. McCLINTOCK, F. A., Trans. ASME (J. Appl. Mech.), 35, 1968, 363.

Table 1 Analyses of Steels, Wt. Pct.

Steel	C	Mn	Mo	Nb	Ni	Cr	Cu	Si	Al	S	Ce	La
Lab., no RE	.040	1.82	.29	.07	.07	.03	-	.17	.05	<.005	-	-
Lab., +RE	.041	1.89	.28	.07	.08	.05	-	.22	.06	<.005	.016	.004
Comm. Mn-Mo-Nb	.046	2.1	.29	.07	.13	.05	.17	.10	.07	.003	.011	-

Table 2 Tensile Data

	Yield Stress, MPa	Ultimate Stress, MPa	Pct. Elong.	Pct. Reduction in Area
Lab., no RE (transverse)	438*	594	25	73
Lab., no RE (long.)	421*	592	27	74
Lab. + RE (transverse)	428*	617	25	73
Lab. + RE (long.)	449*	619	25	72
Comm. Mn-Mo-Nb (transverse)	505**	716	37	60

*0.2 pct. offset yield stress
**0.5 pct. offset yield stress

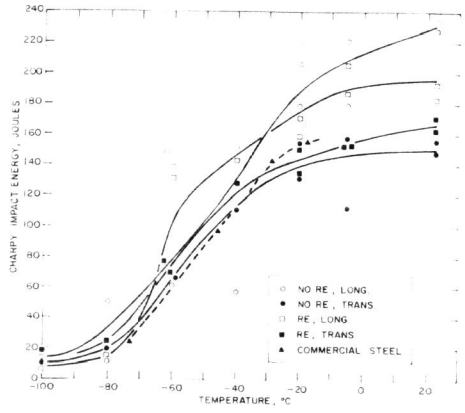

Figure 1 Impact Energy Transition Curves

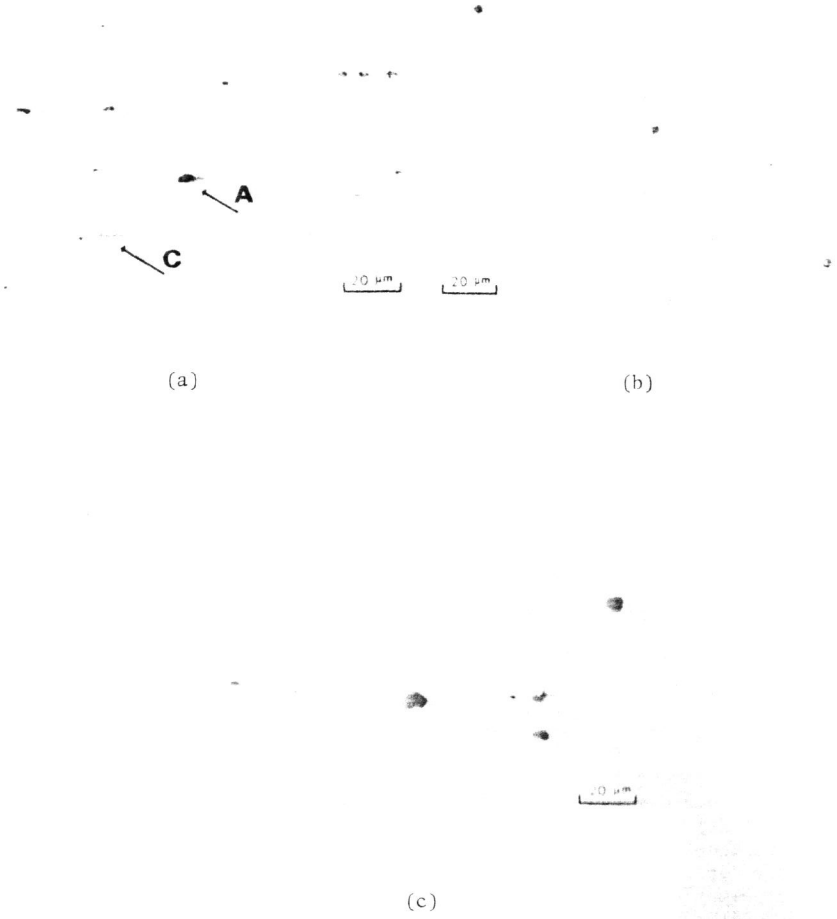

(a) (b)

(c)

Figure 2 Optical Micrographs Showing Typical Inclusion Distributions
(a) Untreated Steel
(b) RE-Treated Steel
(c) Commercial Mn-Mo-Nb Steel

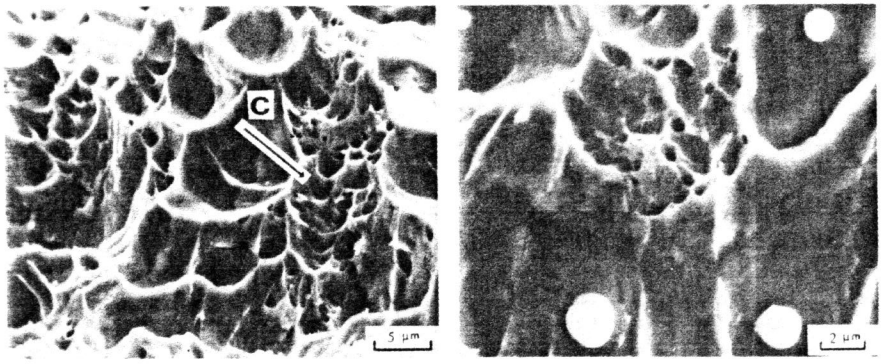

(a) (b)

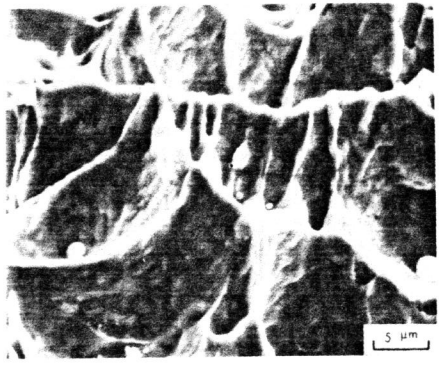

(c)

Figure 3 Scanning Electron Micrographs of Fracture Surfaces

(a) Untreated Steel, Transverse Charpy
(b) RE-Treated Steel, Transverse Tensile
(c) RE-Treated Steel, Transverse Charpy

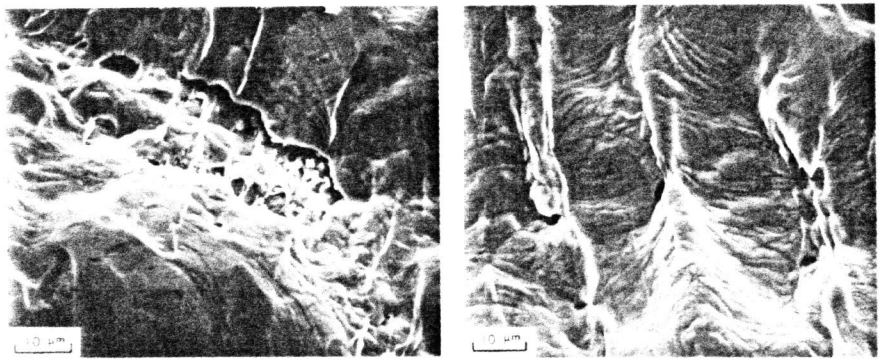

(a) (b)

Figure 4 Scanning Electron Micrographs of Polished Surfaces of Tensile Specimens Taken in Necked Region

(a) RE-Treated Steel
(b) Untreated Steel